Neuronal nitric oxide synthase generates superoxide from the oxygenase domain

Hirohito YONEYAMA, Akira YAMAMOTO and Hiroaki KOSAKA[1]

The Second Department of Physiology, Kagawa Medical University, Miki-cho, Kita-gun, Kagawa 761-0793, Japan

When L-arginine is depleted, neuronal nitric oxide synthase (nNOS) has been reported to generate superoxide. A flavoprotein module construct of nNOS has been demonstrated to be sufficient for superoxide production. In contrast, nNOS was reported not to be involved in superoxide formation, because such formation occurred with a mixture of the boiled enzyme and redox-active cofactors. We aimed to resolve these controversial issues by examining superoxide generation, without the addition of redox-active cofactors, by recombinant wild-type nNOS and by C415A-nNOS, which has a mutation in the haem proximal site. In a superoxide-sensitive adrenochrome assay, the initial lag period of C415A-nNOS was increased 2-fold compared with that of native nNOS. With ESR using the spin trap 5,5-dimethyl-1-pyrroline-*N*-oxide, prominent signals of the superoxide adduct were obtained with wild-type nNOS, whereas an enzyme preparation boiled for 5 min did not produce superoxide. Higher concentrations of NaCN (10 mM) decreased superoxide formation by 63 %. Although the activity of the reductase domain was intact, superoxide generation from C415A-nNOS was decreased markedly, to only 10 % of that of the wild-type enzyme. These results demonstrate that nNOS truly catalyses superoxide formation, that this involves the oxygenase domain, and that full-length nNOS hinders the reductase domain from producing superoxide.

Key words: adrenochrome, C415A-nNOS, DMPO, ESR spin trap, reductase.

INTRODUCTION

Nitric oxide (NO) is produced by a family of homodimeric enzymes termed the NO synthases (NOSs) [1,2]. Three distinct isoforms of NOS, neuronal (nNOS), inducible (iNOS) and endothelial (eNOS), are functionally divided into an N-terminal haem-containing oxygenase domain and a C-terminal FAD- and FMN-containing reductase domain, separated by the putative calmodulin (CaM) binding sequence [3]. Binding of Ca^{2+}/CaM turns on electron flow from NADPH through the reductase domain to the oxygenase domain, where L-arginine is oxidized to form L-citrulline and NO.

In addition to synthesizing NO, all NOS isoforms catalyse superoxide formation under particular conditions [4–6]. Superoxide reacts with NO at a near-diffusion-limited rate ($6.7 \times 10^9\ M^{-1} \cdot s^{-1}$) to form peroxynitrite ($ONOO^-$), which is highly reactive with various biological molecules, and at least partly responsible for the immune function of macrophages [7]. Alteration of NOS activity in favour of superoxide formation is thought to underlie some pathophysiological events involving endothelial dysfunction, e.g. diabetes, atherosclerosis and aging [8].

Previous studies with iNOS have shown that superoxide production was blocked by the flavoprotein inhibitor diphenyleneiodonium (DPI), but not by the haem blocker cyanide (0.1 mM), suggesting that this isoform produces superoxide at the reductase domain [6]. In contrast, eNOS was shown to form superoxide at the oxygenase domain, as superoxide formation was shown to be a Ca^{2+}/CaM-dependent process and was inhibited by the haem blocker sodium cyanide (0.1 mM) [9]. These differences with regard to the site of superoxide generation may influence the pathophysiological roles of the different NOS isoenzymes. Superoxide generation from the iNOS reductase domain is not affected by 0.1 mM L-arginine, strongly suggesting that superoxide and NO synthesis can occur simultaneously within iNOS, resulting in the formation of $ONOO^-$ [6]. Thus this isoform is characterized by its superoxide/$ONOO^-$ generation and contributes to the cytostatic/cytotoxic actions of macrophages in inflammation [7]. Superoxide formation by the eNOS oxygenase domain is prevented by tetrahydrobiopterin (BH_4), which has a binding site on the oxygenase domain [5,10]. Modulation of the BH_4 concentration regulates the proportions of superoxide and NO generated by eNOS *in vitro*. NO and superoxide are involved in ischaemic brain injury, where nNOS is a key molecule [11,12]. As with other isoforms, the mechanism and locus of superoxide secretion in nNOS will be related to its pathophysiological role.

Miller et al. [13] reported that the reductase domain is both necessary and sufficient for superoxide production by nNOS. They showed using an adrenochrome assay that a flavoprotein module construct, which lacks the oxygenase domain, and the mutant enzyme C331A-nNOS, which cannot transfer electrons rapidly to the oxygenase domain, both produced superoxide. However, the question remains as to whether the function of the flavoprotein module construct is physiologically equivalent to that of wild type. Furthermore, superoxide production by C331A-nNOS is decreased compared with that by wild-type nNOS (WT-nNOS). Meanwhile, another report suggested that super-

Abbreviations used: $ONOO^-$, peroxynitrite; NOS, nitric oxide synthase; eNOS, endothelial NOS; iNOS, inducible NOS; nNOS, neuronal NOS; WT-nNOS, wild-type nNOS; CaM, calmodulin; DMPO, 5,5-dimethyl-1-pyrroline-*N*-oxide; DTPA, diethylenetriaminepenta-acetic acid; BH_4, tetrahydrobiopterin; DPI, diphenyleneiodonium.

[1] To whom correspondence should be addressed (e-mail hkosaka@kms.ac.jp).

oxide formation takes place at the oxygenase domain of nNOS, as NaCN was inhibitory [14]. However, the concentration of NaCN required to block superoxide generation from nNOS (EC_{50} = 10 mM) was three orders of magnitude greater than for eNOS (for which 0.1 mM NaCN resulted in > 80 % inhibition). Surprisingly, it was recently reported that nNOS does not catalyse superoxide formation [15,16].

We have focused on determining whether the reductase domain or the oxygenase domain is responsible for superoxide generation by nNOS. To this end, we constructed a C415A mutant of nNOS, which has a mutation of the axial haem ligand cysteine-415, resulting in loss of the catalytic function of haem. However, the full-length construct C415A-nNOS shows the same native global folding as WT-nNOS [17], and is expected to retain physiological reductase domain functioning. In the present study, we performed adrenochrome assays and ESR spin trapping using WT- and C415A-nNOS.

EXPERIMENTAL

Materials

Mouse nNOS/pSG5 [18], containing mouse nNOS cDNA in pSG5, was kindly provided by Hiroyasu Esumi and Tsutomu Ogura (National Cancer Center Research Institute, Tokyo, Japan). pKY206 [19], containing GroES and GroEL cDNAs in pACYC184, and pSAR [20], containing sheep ferredoxin reductase cDNA in pCW, were generously donated by Koreaki Ito and Yoshinori Akiyama (Institute for Virus Research, Kyoto University, Kyoto, Japan) and Aizo Furukawa (Kagawa Medical University, Kagawa, Japan) respectively. 5,5-Dimethyl-1-pyrroline-*N*-oxide (DMPO) was purchased from Dojindo Laboratory (Kumamoto, Japan); catalase was from Boehringer (Mannheim, Germany); superoxide dismutase was from Sigma (St Louis, MO, U.S.A.); NADPH, BH_4 [(6*R*)-5,6,7,8-tetrahydro-L-biopterin], L- and D-arginine, sodium cyanide (NaCN), DPI and all other chemicals were from Wako Pure Chemicals (Osaka, Japan). CaM was purified from pig brains as described previously [21].

Recombinant DNA manipulations

The first 901 bp of mouse nNOS (from the ATG start codon to the *Afl*II restriction site) were amplified by PCR using mouse nNOS/pSG5 as template. The primers used were 5′-catatggaagagcacacgtttggggtcc-3′ and 5′-tctagaccttaaggaagcgagggcacctg-3′. The PCR product was gel-purified and cloned into pCW as an *Nde*I–*Xba*I fragment (pYH01). The remainder of the nNOS coding sequence was generated from mouse nNOS/pSG5 as an *Afl*II–*Xba*I fragment and cloned into pYH01 (WT-nNOSpCW). The PCR-generated portion of WT-nNOSpCW was sequenced and verified against the reported sequence (GenBank accession no. NM 008712).

The desired mutation [codon at position 1243: TGT (cysteine) changed to GCT (alanine)] was introduced by PCR with the primer set 5′-accaagaatggcagtccttc-3′ and 5′-cactggatcctgcccacAGCgcgagaggcgtt-3′, using WT-nNOSpCW as template. The amplified mutated fragment representing positions 866–1262 was cloned into WT-nNOSpCW (C415A-nNOSpCW).

GroEL/ES coding sequences in pKY206 were cloned into pLysE (Novagen) as a *Hin*dIII–*Hin*dIII fragment, yielding the plasmid pLysGroELS for the expression of GroES and GroEL.

Enzyme preparation

pLysGroELS and either WT-nNOSpCW or C415A-nNOSpCW were co-transfected into *Escherichia coli* BLR cells by electroporation. Under selective pressure (50 μg/ml ampicillin and 35 μg/ml chloramphenicol), overexpression of WT-nNOS or C415A-nNOS in BLR was performed as described previously [22]. WT- or C415A-nNOS was purified from harvested cells by 2′,5′-ADP–Sepharose and CaM–Sepharose affinity chromatography as described previously [23]. On SDS/PAGE, the purified protein preparations exhibited a prominent major band (> 90 % pure) at the expected 150 kDa position. Protein concentrations were determined by the Bradford protein assay using BSA as a standard [24]. Visible absorption spectra of purified enzymes were recorded at 15 °C and their haem content was measured by the pyridine haemochromogen method [25]. BH_4 content in the recombinant nNOS preparation was measured by HPLC with fluorescence detection after oxidation with KI/I_2 in acid and alkali as described previously [26].

Measurement of nNOS activity

The catalytic activity of nNOS was determined by measuring the conversion of L-[^{14}C]arginine into L-[^{14}C]citrulline at 37 °C as described previously [27]. When we investigated the effect of NaCN on nNOS activity, NO production by the enzyme was determined as nitrite. After a 5 min incubation at 37 °C, the reaction was terminated by the addition of 5 mM EGTA, and the reaction mixture was analysed using the Griess reagent [12].

The NADPH-dependent reduction of cytochrome *c* and ferricyanide by nNOS was followed spectrophotometrically at 37 °C in 1 ml of Tris/HCl buffer (50 mM, pH 7.4) containing 10 nM nNOS, 150 μM NADPH, 1 mM $CaCl_2$ and either 50 μM cytochrome *c* or 0.9 mM potassium ferricyanide, with or without 0.1 mg/ml CaM. The rates of reduction of cytochrome *c* and ferricyanide were followed at 550 nm (ϵ_{550} 21 $mM^{-1} \cdot cm^{-1}$) and 420 nm (ϵ_{420} 1.2 $mM^{-1} \cdot cm^{-1}$) respectively [28].

Adrenochrome assay

The formation of adrenochrome from adrenaline (epinephrine) was followed spectrophotometrically at 480 nm at 25 °C [13]. Dithiothreitol in the enzyme preparation was removed by gel filtration, as the reducing agent interferes with this assay.

ESR spectroscopy and spin trapping

ESR spin trapping of oxygen free radicals was performed in 50 mM Tris/HCl buffer (pH 7.4) containing 0.1 mM DTPA (diethylenetriaminepenta-acetic acid) and 50 mM DMPO. Reactions were started by adding purified WT- or C415A-nNOS. At 90 s after the addition of NOS, the ESR spectra were recorded at room temperature (22 °C) with a JEOL JES-RE1X spectrometer. Instrument settings were: scan speed, 10 mT/min; time constant, 0.1 s; microwave power, 20 mW; microwave frequency, 9.4 GHz; modulation amplitude, 0.1 mT; receiver gain, 1000.

Statistical analysis

Data are presented as means ± S.D., and were analysed for significance by one-way ANOVA and the Scheffé post hoc test. Values of $P < 0.05$ were considered to be significant.

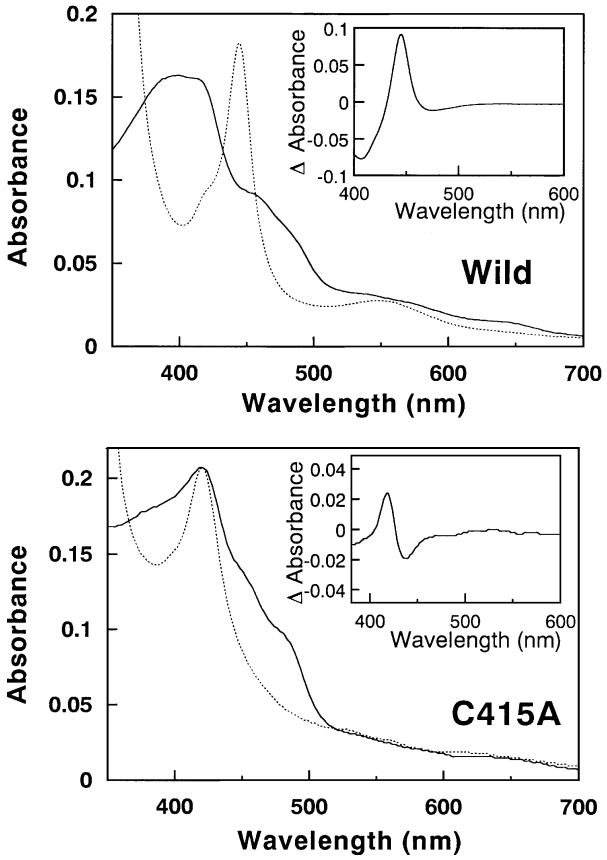

Figure 1 Absolute absorbance and CO difference spectra of purified WT-nNOS and C415A-nNOS at 15 °C

The cuvette contained 1.4 μM enzyme in 20 mM Tris/HCl buffer (pH 7.4). Solid line, resting state; broken line, dithionite-reduced CO state. Inset: difference spectrum of CO-complex minus reduced state.

Table 1 Catalytic profile of recombinant mouse WT-nNOS purified from an *E. coli* expression system

NOS activity was measured by monitoring the conversion of L-[^{14}C]arginine into L-[^{14}C]citrulline at 37 °C. The control mixture consisted of 27 nM nNOS, 0.1 mg/ml CaM, 1 mM NADPH, 20 μM L-arginine, 10 μM BH_4, 10 μM oxyhaemoglobin, 1 mg/ml BSA and 0.2 mM $CaCl_2$. L-NAME, N^{ω}-nitro-L-arginine methyl ester. Values are means ± S.D. ($n = 4$). Significance of differences: $^*P < 0.0001$ compared with control.

Experimental conditions	k_{cat} (min^{-1})
Control	63.5 ± 4.6
Ca^{2+}-free	2.8 ± 0.6*
CaM-free	3.8 ± 2.2*
+ L-NAME (2 mM)	3.5 ± 0.9*

RESULTS

Spectral and catalytic properties of recombinant WT-nNOS

Recombinant mouse WT-nNOS was expressed in an *E. coli* expression system and purified using affinity chromatography.

Table 2 Cytochrome *c* and ferricyanide reductase activities of WT-nNOS and C415A-nNOS

Purified enzymes (10 nM) were incubated with 50 μM cytochrome *c* or 0.6 mM potassium ferricyanide in Hepes buffer (50 mM, pH 7.4) containing 150 μM NADPH and 1 mM $CaCl_2$. Assays were run at 37 °C in the absence (−) or presence (+) of 0.1 mg/ml CaM. Data are means ± S.D. ($n = 3$).

	Specific activity (μmol of electron acceptor reduced · min^{-1} · mg^{-1})			
	Cytochrome *c*		Ferricyanide	
Enzyme	−CaM	+CaM	−CaM	+CaM
WT-nNOS	1.09 ± 0.01	19.4 ± 0.3	21.6 ± 0.7	30.3 ± 1.6
C415A-nNOS	1.33 ± 0.02	24.0 ± 0.8	27.5 ± 0.4	37.1 ± 0.9

First, we checked the spectral and catalytic properties of the purified WT-nNOS. Figure 1 (upper panel, solid line) shows the absolute spectrum of WT-nNOS. It has absorption maxima at 400, 550 and 650 nm, indicative of a high-spin form. Some low-spin form was also present, as indicated by the shoulder at 410 nm. Shoulders originating from flavin absorbance were also observed at 450 and 475 nm. When WT-nNOS was reduced with dithionite in the presence of CO, the flavin absorbance vanished, revealing a peak at 444 nm (Figure 1, upper panel, broken line). The inset of Figure 1 shows the difference spectrum (CO-complex minus reduced state) of the purified enzyme, with a prominent peak at 444 nm. These spectral characteristics are identical with those of rat nNOS isolated from kidney 293 cells [29].

The k_{cat} for recombinant WT-nNOS, measured as the conversion of L-[^{14}C]arginine into L-[^{14}C]citrulline, was 63.5 ± 4.6 min^{-1}; this is within the range for rat nNOS reported previously [22]. NO synthase activity was dependent on Ca^{2+}/CaM, and was blocked by N^{ω}-nitro-L-arginine methyl ester (Table 1).

Spectral and catalytic properties of recombinant C415A-nNOS mutant

The recombinant mouse C415A-nNOS mutant was prepared in the same way as WT-nNOS. Figure 1 (lower panel, solid line) shows the absolute spectrum of purified C415A-nNOS. It demonstrates an absorbance maximum at 420 nm of unknown origin, but a Soret band in the 400 nm region, a marker of high-spin haem, is absent. The spectrum exhibits shoulders at 450 and 475 nm, indicating that this mutant preserves the flavins in the reductase domain. When the C415A mutant was reduced with dithionite in the presence of CO, the flavin absorbance decreased (Figure 1, lower panel, broken line). The difference spectrum (CO-complex minus reduced state) displayed a small peak at 418 nm, but no significant peak at 444 nm (Figure 1, lower panel, inset). Both the mutant and native nNOS forms were analysed for haem content by the pyridine haemochromogen assay. WT-nNOS contained 1.0 equivalent of haem/subunit, whereas C415A-nNOS contained only 0.1 equivalent of haem/subunit.

The mutant nNOS had no detectable activity for the conversion of L-[^{14}C]arginine into L-[^{14}C]citrulline. However, C415A-nNOS catalysed both the NADPH–cytochrome *c* and NADPH–ferricyanide reductase activities at rates similar to those of WT-nNOS (Table 2). For both WT- and C415A-nNOS, the addition of Ca^{2+}/CaM increased the rates of cytochrome *c* and ferricyanide

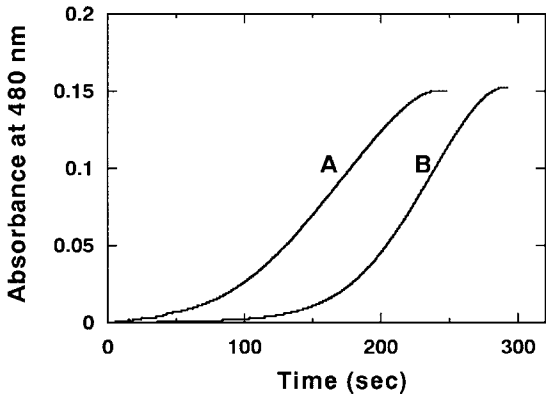

Figure 2 Adrenochrome formation by WT-nNOS and C415A-nNOS

The reaction mixture consisted of 0.2 mM adrenaline, 0.125 μM enzyme, 1 μM CaM, 0.4 mM $CaCl_2$ and 1 mM NADPH. Reactions were run in the presence of 0.125 μM WT-nNOS (trace A) or 0.125 μM C415A-nNOS (trace B) at 25 °C.

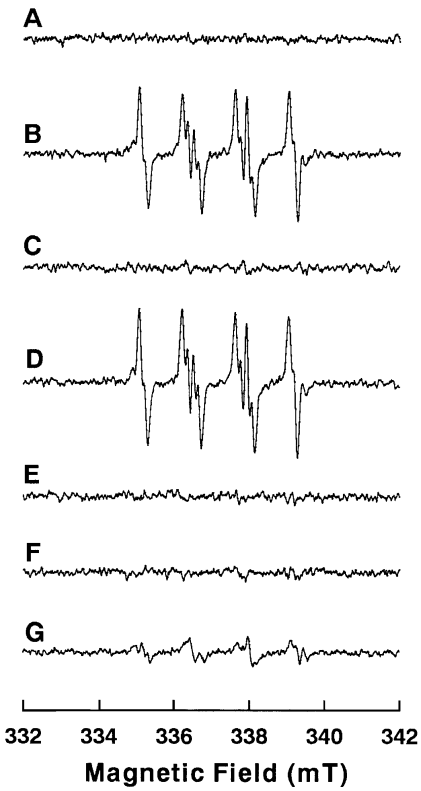

Figure 3 ESR spectra of superoxide spin adduct generated by nNOS

The mixture that resulted in trace B consisted of 0.1 M DMPO, 0.1 mM DTPA, 150 μg/ml CaM, 0.5 mM $CaCl_2$, 1 mM NADPH, 1 mg/ml BSA and 0.65 μM WT-nNOS. No signal was observed from the mixture without WT-nNOS (trace A). Traces C and D were recorded under identical conditions to trace B, except for the addition of 40 units/ml superoxide dismutase and 300 units/ml catalase respectively. For traces E and F, $CaCl_2$ and CaM respectively were omitted from the mixture. Trace G was obtained under the same conditions as for trace B, except that WT-nNOS was replaced with 0.65 μM C415A-nNOS. ESR measurements were obtained 90 s after starting the reaction at 25 °C.

reduction, by factors of 17–18 and 1.3–1.4 respectively. These results demonstrate that purified C415A-nNOS retains the activity of the reductase domain.

Table 3 Effects of boiling of nNOS, or the presence of BH_4, L- or D-arginine or DPI, on superoxide formation by WT-nNOS and C415A-nNOS

Experimental conditions were as described in the legend to Figure 3. Reaction mixtures consisted of 0.1 M DMPO, 0.1 mM DTPA, 150 μg/ml CaM, 0.5 mM $CaCl_2$, 1 mM NADPH, 1 mg/ml BSA and 0.65 μM WT-nNOS or C415A-nNOS. For boiling, nNOS was heat-denatured for 5 min at 100 °C. Data are means ± S.D. ($n = 4$). Significance of differences: *$P < 0.0001$ compared with respective WT-nNOS value; †$P < 0.0005$ compared with respective control value.

	Intensity of DMPO-OOH signal (arbitrary units)	
Treatment	WT-nNOS	C415A-nNOS
None (control)	35.0 ± 1.0	3.8 ± 0.3*
Boiled enzyme	0.5 ± 0.2†	0.2 ± 0.1†
+ 10 μM BH_4	13.8 ± 1.2†	3.7 ± 0.5*
+ 0.1 mM L-arginine	10.6 ± 0.6†	4.0 ± 0.4*
+ 0.1 mM D-arginine	34.7 ± 1.7	3.6 ± 0.3*
+ 20 μM DPI	0.8 ± 0.6†	0.2 ± 0.1†

Adrenochrome assay

A previous study by Miller et al. [13] reported superoxide production by a flavoprotein module construct and by the mutant C331A-nNOS, which does not transfer NADPH-derived electrons efficiently to the haem iron, and concluded that the reductase domain is necessary and sufficient for superoxide generation. That study [13] employed the adrenochrome assay for detection of superoxide. We examined whether similar amounts of superoxide were generated from WT- and C415A-nNOS using the adrenochrome assay. Two distinct phases were evident in the conversion of adrenaline into adrenochrome by WT-nNOS (Figure 2, trace A), as described previously [13]. The early period (phase I) is the initial lag period, during which enzymically formed superoxide oxidizes adrenaline to adrenaline semiquinone and adrenaline *o*-quinone, which is autoxidized rapidly to adrenochrome accompanying O_2 reduction to superoxide. On adrenochrome accumulation, phase I is succeeded by the rapid phase II: the reductase domain of nNOS reduces adrenochrome back to the quinone intermediate by consuming NADPH, which is then autoxidized again, accompanying enhanced superoxide formation due to redox cycling, leading to an accelerated rate of adrenochrome formation. The rate of phase II mainly reflects the activity of the reductase domain of nNOS. The rate of phase I should be proportional to the rate of enzyme-mediated superoxide formation. Although the rate of the rapid redox-cycling phase II of adrenochrome formation with C415A-nNOS was similar to that with native nNOS, phase I was prolonged for C415A-nNOS (Figure 2, trace B) compared with that seen with WT-nNOS (Figure 2, trace A), suggesting that superoxide production in the mutant enzyme is markedly slower than in native nNOS. These results suggest the possibility that superoxide is generated by the oxygenase domain of nNOS.

Spin-trapping experiment

To address this issue further, we applied an ESR spin-trapping technique using DMPO to quantify superoxide generation from nNOS directly. No signals were detected in the ESR spectrum of the reaction mixture devoid of nNOS (Figure 3, trace A). Strong ESR signals were observed in a reaction mixture containing 0.65 μM purified WT-nNOS in the absence of L-arginine (Figure

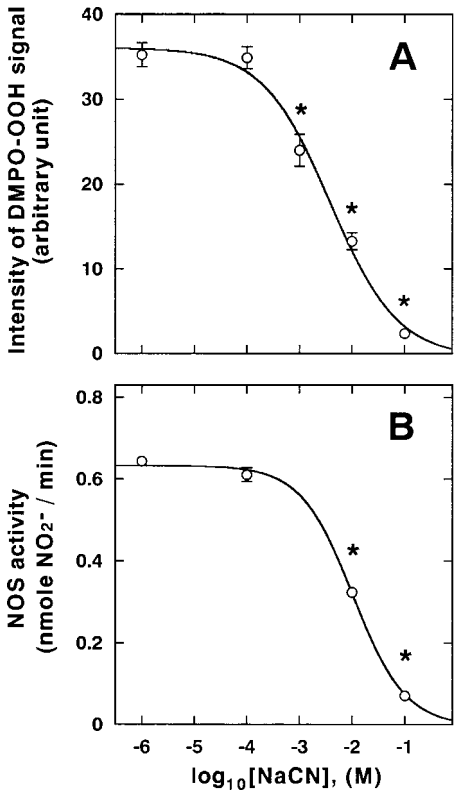

Figure 4 Effects of NaCN on superoxide and NO production by nNOS

(**A**) Effect of NaCN on superoxide formation by nNOS. Experimental conditions were as in Figure 3. Data represent relative signal heights of the DMPO-OOH spin adduct in the presence of NaCN at the concentrations indicated. (**B**) Effect of NaCN on nNOS activity. The activity was monitored by measuring NO_2^- in the reaction mixture after a 5 min incubation at 37 °C. The mixture consisted of 50 nM nNOS, 0.1 mg/ml CaM, 1 mM NADPH, 20 μM L-arginine, 10 μM BH_4, 1 mg/ml BSA, 0.2 mM $CaCl_2$ and NaCN at the concentrations indicated. Data are means $\pm$ S.D. ($n = 4$). Significance of differences: $^*P < 0.0001$ compared with mixture without NaCN.

3, trace B). These signals, showing the characteristic DMPO-OOH adduct ($a_N = 1.40$ mT, $a_{H^\beta} = 1.16$ mT, $a_{H^\gamma} = 0.12$ mT), were abolished by superoxide dismutase (40 units/ml), but not by catalase (300 units/ml) (Figure 3, traces C and D respectively). Omission of Ca^{2+} or CaM eliminated the ESR signals (Figure 3, traces E and F respectively). Recently, Xu [15,16] observed superoxide generation from a reaction mixture containing boiled nNOS, FAD, FMN, NADPH, BH_4 and CaM; he concluded that superoxide generation resulted from autoxidation of redox-active cofactors, and that NOS does not catalyse superoxide formation. In our assay, FAD and FMN were not added throughout. The enzyme preparation boiled for 5 min did not produce superoxide (Table 3), proving that the superoxide formation in our experiments was not due to a non-enzymic reaction. The observed signal formation was inhibited (39%) by the addition of 10 μM BH_4 (Table 3). Our result with BH_4 is similar to that of Vasquez Vivar et al. [30], since the purified protein as isolated is BH_4-free due to the absence of GTP hydroxylase in *E. coli*, while the enzyme isolated from eukaryotic cells may contain tightly bound BH_4 [31]. We did not detect BH_4 in either purified WT- or C415A-nNOS (0.2 μM each) (the detection limit of BH_4 was < 0.5 nM). The observed signal formation was inhibited by the addition of 0.1 mM L-arginine (30%), but not by its non-substrate enantiomer D-arginine (Table 3).

Effects of DPI and NaCN

There are two possible sites on nNOS where superoxide formation could occur: the flavins (FAD and FMN) and the haem iron. DPI at 20 μM diminished WT-nNOS-mediated superoxide formation (Table 3). This result merely indicates that the electrons used for superoxide formation flowed through the flavins, since the NADPH-derived electron flows from the reductase domain to the haem-containing oxygenase domain. To address whether the haem site is responsible for O_2 reduction, we investigated the effect of 0.1 mM NaCN on superoxide generation by nNOS. NaCN at 0.1 mM was reported previously to be effective in a similar experiment with eNOS [9], but was not effective with nNOS in the present study (Figure 4A). However, NaCN concentrations greater than 1 mM decreased the peak height of DMPO-OOH (Figure 4A) and NO (Figure 4B) formation by nNOS. IC_{50} values of 3.4 ± 0.6 and 10.5 ± 1.5 mM were observed for superoxide and NO generation respectively. These results are consistent with those obtained with the adrenochrome assay.

Superoxide generation from WT-nNOS and C415A-nNOS

To confirm a role for the oxygenase domain in superoxide formation directly, we compared the ESR spin-trapping adduct of DMPO from WT- and C415A-nNOS. DMPO-OOH signal formation from the mutant was only 10% of that from WT-nNOS (Figure 3, trace G). The observed signal formation from the mutant was not inhibited by the addition of 10 μM BH_4 or 0.1 mM L-/D-arginine (Table 3). Boiling of C415A-nNOS or addition of 20 μM DPI diminished the DMPO-OOH signal from the mutant enzyme (Table 3).

DISCUSSION

In the present study, we aimed to determine which domain is responsible for superoxide generation from nNOS. To this end, we constructed C415A-nNOS, a full-length construct; this mutant has a mutation in the haem binding proximal site, but its reductase domain is physiologically intact. Indeed, the reductase domain activities, i.e. NADPH–cytochrome *c* and NADPH–ferricyanide reductase activities, were intact in C415A-nNOS. In an adrenochrome assay, the late rapid phase for C415A-nNOS was similar to that for WT-nNOS, suggesting that the redox-cycling activity of the reductase domain is intact in the mutant. However, the initial lag period for C415A-nNOS was 2-fold longer than that for WT-nNOS, suggesting the possibility that superoxide generation was decreased in C415A-nNOS. Next we quantified the effect by an ESR spin-trapping technique. We demonstrate here for the first time that superoxide formation by C415A-nNOS was decreased to 10% of that by WT-nNOS. These results show that the oxygenase domain of nNOS is responsible for superoxide formation.

The adrenochrome assay has been shown to be useful for the analysis of superoxide formation by NOS [13]. Using this method, Miller et al. [13] succeeded in demonstrating superoxide production by nNOS during catalytic turnover. They suggested that the reductase domain is essential and sufficient for superoxide production, because both a flavoprotein module construct and C331A-nNOS (which does not transfer electrons to the haem iron efficiently) produced superoxide, as assessed using the adrenochrome assay [13]. However, we demonstrated that superoxide generation by BH_4-free C415A-nNOS, which has intact reductase activity, was decreased to 10% of that in the wild-type enzyme. Although the reason for the difference in the evaluation of superoxide formation by the different methods is unclear, ESR

spin trapping is believed to be a reliable direct method. The adrenochrome formation rate should be proportional to the amount of superoxide; however, this might not be the case when the reductase domain of nNOS reduces adrenochrome back to quinone, which would amplify superoxide generation, as pointed out by Miller et al. [13].

The mutant C331A-nNOS was reported to be catalytically incompetent and not to bind BH_4. However, upon prolonged incubation with L-arginine, not only BH_4 binding but also catalytic activity could be restored. The K_d value for L-arginine of C331A-nNOS is much higher than that of the native enzyme (0.1 mM compared with 2–3 μM). C331A-nNOS retains the haem at the proximal binding site, and binding of L-arginine to the enzyme is slow. L-Arginine promotes the transition of haem iron from a low- to a high-spin state. In contrast, binding of the haem ligand imidazole, which forms the low-spin state alone, was indistinguishable between C331A- and WT-nNOS. Although the rate of electron flow to haem is low in C331A-nNOS, oxygen must be able to bind in part to the haem, because CO can bind in part to the haem [32]. This may be the reason why BH_4-free C331A-nNOS generated superoxide levels of 31 % of those with WT-nNOS, as measured using an ESR spin-trapping technique [30].

Another unresolved issue is the report that a reductase construct of nNOS, lacking the oxygenase domain, produced superoxide in a Ca^{2+}/CaM-independent manner [13]. In this regard, it is notable that the reductase domain of nNOS possesses an auto-inhibitory control element whose docking with a site on the enzyme impedes CaM binding and thus enzymic activation, due to a conformational change [33]. Although the location and identity of the sites of interaction with the inhibitory unit are not fully known, a site on the oxygenase domain is presumed to be one of the targets. Since the C415A mutant retains native global folding [17], the function of the reductase domain must be under the control of the Ca^{2+}/CaM switch, as shown by the activation of NADPH–cytochrome *c* and NADPH–ferricyanide reductase activities after stimulation with Ca^{2+}/CaM. Thus it can be assumed that deletion of the oxygenase domain will result in accelerated, CaM-independent and uncontrolled electron transfer in the reductase domain, unlike the situation in native nNOS. The origin of the 10 % superoxide production by C415A-nNOS is uncertain. Because boiling or addition of DPI inhibited superoxide formation by the mutant, it appears to depend on enzyme-catalysed electron transport. Although BH_4 and L-arginine did not inhibit DMPO-OOH signal formation in C415A-nNOS, this does not necessarily exclude a role for the oxygenase domain in superoxide production, because the mutant could not execute NO synthesis, and it is uncertain whether the cofactor and substrate are in appropriate positions. Either the small amount of catalytically inert haem in the mutant or an electron leak from the reductase domain may account for the superoxide production that remains.

Our results demonstrate that superoxide formation by nNOS is not due to non-enzymic autoxidation of redox-active cofactors, and that 90 % of superoxide formation originates from haem in the oxygenase domain of nNOS. The present study also suggested that decreases in BH_4 and L-arginine, which would not occur in the physiological state, induce superoxide generation from nNOS. In this regard, we have recently observed that L-arginine improved endothelial function in the renal artery and blood pressure in hypertensive Dahl rats [34]. Whether superoxide generation from NOS under conditions of BH_4 and L-arginine deficiency has an important pathophysiological role, e.g. activation of cell signalling pathways leading to cell proliferation [35], remains to be determined.

This research was supported in part by Grants-in-Aid from the Ministry of Education, Science and Culture of Japan.

REFERENCES

1 Nathan, C. and Xie, Q. W. (1994) Nitric oxide synthases: roles, tolls, and controls. Cell **78**, 915–918

2 Yoneyama, H., Kosaka, H., Ohnishi, T., Kawazoe, T., Mizoguchi, K. and Ichikawa, Y. (1999) Reaction of neuronal nitric oxide synthase with the nitric oxide spin-trapping agent, iron complexed with N-dithiocarboxysarcosine. Eur. J. Biochem. **266**, 771–777

3 Masters, B. S., McMillan, K., Sheta, E. A., Nishimura, J. S., Roman, L. J. and Martasek, P. (1996) Neuronal nitric oxide synthase, a modular enzyme formed by convergent evolution: structure studies of a cysteine thiolate-liganded heme protein that hydroxylates L-arginine to produce NO as a cellular signal. FASEB J. **10**, 552–558

4 Pou, S., Pou, W. S., Bredt, D. S., Snyder, S. H. and Rosen, G. M. (1992) Generation of superoxide by purified brain nitric oxide synthase. J. Biol. Chem. **267**, 24173–24176

5 Vasquez Vivar, J., Kalyanaraman, B., Martasek, P., Hogg, N., Masters, B. S., Karoui, H., Tordo, P. and Pritchard, Jr, K. A. (1998) Superoxide generation by endothelial nitric oxide synthase: the influence of cofactors. Proc. Natl. Acad. Sci. U.S.A. **95**, 9220–9225

6 Xia, Y., Roman, L. J., Masters, B. S. and Zweier, J. L. (1998) Inducible nitric-oxide synthase generates superoxide from the reductase domain. J. Biol. Chem. **273**, 22635–22639

7 Xia, Y. and Zweier, J. L. (1997) Superoxide and peroxynitrite generation from inducible nitric oxide synthase in macrophages. Proc. Natl. Acad. Sci. U.S.A. **94**, 6954–6958

8 Benkusky, N. A., Lewis, S. J. and Kooy, N. W. (1999) Peroxynitrite-mediated attenuation of alpha- and beta-adrenoceptor agonist-induced vascular responses in vivo. Eur. J. Pharmacol. **364**, 151–158

9 Xia, Y., Tsai, A. L., Berka, V. and Zweier, J. L. (1998) Superoxide generation from endothelial nitric-oxide synthase. A Ca^{2+}/calmodulin-dependent and tetrahydrobiopterin regulatory process. J. Biol. Chem. **273**, 25804–25808

10 Raman, C. S., Li, H., Martasek, P., Kral, V., Masters, B. S. and Poulos, T. L. (1998) Crystal structure of constitutive endothelial nitric oxide synthase: a paradigm for pterin function involving a novel metal center. Cell **95**, 939–950

11 Zhang, Z. G., Chopp, M., Gautam, S., Zaloga, C., Zhang, R. L., Schmidt, H. H., Pollock, J. S. and Forstermann, U. (1994) Upregulation of neuronal nitric oxide synthase and mRNA, and selective sparing of nitric oxide synthase-containing neurons after focal cerebral ischemia in rat. Brain Res. **654**, 85–95

12 Kumura, E., Yoshimine, T., Iwatsuki, K. I., Yamanaka, K., Tanaka, S., Hayakawa, T., Shiga, T. and Kosaka, H. (1996) Generation of nitric oxide and superoxide during reperfusion after focal cerebral ischemia in rats. Am. J. Physiol. **270**, C748–C752

13 Miller, R. T., Martasek, P., Roman, L. J., Nishimura, J. S. and Masters, B. S. (1997) Involvement of the reductase domain of neuronal nitric oxide synthase in superoxide anion production. Biochemistry **36**, 15277–15284

14 Pou, S., Keaton, L., Surichamorn, W. and Rosen, G. M. (1999) Mechanism of superoxide generation by neuronal nitric-oxide synthase. J. Biol. Chem. **274**, 9573–9580

15 Xu, K. Y. (2000) Does nitric oxide synthase catalyze the synthesis of superoxide? FEBS Lett. **474**, 252–253

16 Xu, K. Y. (2000) A key negative control experiment provides evidence that nitric oxide synthase does not catalyze superoxide formation. FEBS Lett. **481**, 306–307

17 Richards, M. K., Clague, M. J. and Marletta, M. A. (1996) Characterization of C415 mutants of neuronal nitric oxide synthase. Biochemistry **35**, 7772–7780

18 Ogura, T., Yokoyama, T., Fujisawa, H., Kurashima, Y. and Esumi, H. (1993) Structural diversity of neuronal nitric oxide synthase mRNA in the nervous system. Biochem. Biophys. Res. Commun. **193**, 1014–1022

19 Ito, K. and Akiyama, Y. (1991) In vivo analysis of integration of membrane proteins in Escherichia coli. Mol. Microbiol. **5**, 2243–2253

20 Furukawa, A., Okuyama, E., Sumi, T. and Ichikawa, Y. (1997) Molecular cloning of sheep and goat ferredoxin reductase messenger ribonucleic acids, and identification of an alternatively spliced form of sheep ferredoxin reductase. Biol. Reprod. **56**, 1336–1342

21 Yazawa, M., Sakuma, M. and Yagi, K. (1980) Calmodulins from muscles of marine invertebrates, scallop and sea anemone. J. Biochem. (Tokyo) **87**, 1313–1320

22 Roman, L. J., Sheta, E. A., Martasek, P., Gross, S. S., Liu, Q. and Masters, B. S. (1995) High-level expression of functional rat neuronal nitric oxide synthase in Escherichia coli. Proc. Natl. Acad. Sci. U.S.A. **92**, 8428–8432

23 Mayer, B., Klatt, P., List, B. M., Harteneck, C. and Schmidt, K. (1996) Large-scale purification of rat brain nitric oxide synthase from Baculovirus overexpression system. Methods Enzymol. **268**, 420–427

24 Bradford, M. M. (1976) A rapid and sensitive method for the quantitation of microgram quantities of protein utilizing the principle of protein-dye binding. Anal. Biochem. **72**, 248–254
25 Berry, E. A. and Trumpower, B. L. (1987) Simultaneous determination of hemes a, b, and c from pyridine hemochrome spectra. Anal. Biochem. **161**, 1–15
26 Klatt, P., Schmidt, K., Werner, E. R. and Mayer, B. (1996) Determination of nitric oxide synthase cofactors. Methods Enzymol. **268**, 358–365
27 Kumar, V. B., Bernardo, A. E., Alshaher, M. M., Buddhiraju, M., Purushothaman, R. and Morley, J. E. (1999) Rapid assay for nitric oxide synthase using thin-layer chromatography. Anal. Biochem. **269**, 17–20
28 Ostrowski, J., Barber, M. J., Rueger, D. C., Miller, B. E., Siegel, L. M. and Kredich, N. M. (1989) Characterization of the flavoprotein moieties of NADPH-sulfite reductase from Salmonella typhimurium and Escherichia coli. Physicochemical and catalytic properties, amino acid sequence deduced from DNA sequence of cysJ, and comparison with NADPH-cytochrome P-450 reductase. J. Biol. Chem. **264**, 15796–15808
29 McMillan, K., Bredt, D. S., Hirsch, D. J., Snyder, S. H., Clark, J. E. and Masters, B. S. (1992) Cloned, expressed rat cerebellar nitric oxide synthase contains stoichiometric amounts of heme, which binds carbon monoxide. Proc. Natl. Acad. Sci. U.S.A. **89**, 11141–11145
30 Vasquez Vivar, J., Hogg, N., Martasek, P., Karoui, H., Pritchard, Jr, K. A. and Kalyanaraman, B. (1999) Tetrahydrobiopterin-dependent inhibition of superoxide generation from neuronal nitric oxide synthase. J. Biol. Chem. **274**, 26736–26742
31 Gorren, A. C., List, B. M., Schrammel, A., Pitters, E., Hemmens, B., Werner, E. R., Schmidt, K. and Mayer, B. (1996) Tetrahydrobiopterin-free neuronal nitric oxide synthase: evidence for two identical highly anticooperative pteridine binding sites. Biochemistry **35**, 16735–16745
32 Martasek, P., Miller, R. T., Liu, Q., Roman, L. J., Salerno, J. C., Migita, C. T., Raman, C. S., Gross, S. S., Ikeda Saito, M. and Masters, B. S. (1998) The C331A mutant of neuronal nitric-oxide synthase is defective in arginine binding. J. Biol. Chem. **273**, 34799–34805
33 Salerno, J. C., Harris, D. E., Irizarry, K., Patel, B., Morales, A. J., Smith, S. M., Martasek, P., Roman, L. J., Masters, B. S., Jones, C. L. et al. (1997) An autoinhibitory control element defines calcium-regulated isoforms of nitric oxide synthase. J. Biol. Chem. **272**, 29769–29777
34 Zhou, M., Kosaka, H., Tian, R., Abe, Y., Chen, Q., Yoneyama, H., Yamamoto, A. and Zhang, L. (2001) L-Arginine improves endothelial function in renal artery of hypertensive Dahl rats. J. Hypertens. **19**, 421–429
35 Li, H. and Forstermann, U. (2000) Nitric oxide in the pathogenesis of vascular disease. J. Pathol. **190**, 244–254

Received 18 June 2001/16 August 2001; accepted 19 September 2001